CHIN. PHYS. LETT. Vol. 35, No. 4 (2018) 047301

Nonvolatile Resistive Switching and Physical Mechanism in $LaCrO_3$ Thin Films *

Wan-Jing Hu(胡万景)[1,2], Ling Hu(胡令)[1**], Ren-Huai Wei(魏仁怀)[1], Xian-Wu Tang(汤现武)[1], Wen-Hai Song(宋文海)[1], Jian-Ming Dai(戴建明)[1], Xue-Bin Zhu(朱雪斌)[1**], Yu-Ping Sun(孙玉平)[1,3,4]

[1]*Key Laboratory of Materials Physics, Institute of Solid State Physics, Chinese Academy of Sciences, Hefei 230031*
[2]*University of Science and Technology of China, Hefei 230026*
[3]*High Magnetic Field Laboratory, Chinese Academy of Sciences, Hefei 230031*
[4]*Collaborative Innovation Center of Advanced Microstructures, Nanjing University, Nanjing 210093*

(Received 11 January 2018)

Polycrystalline $LaCrO_3$ (LCO) thin films are deposited on $Pt/Ti/SiO_2/Si$ substrates by pulsed laser deposition and used as the switching material to construct resistive random access memory devices. The unipolar resistive switching (RS) behavior in the Au/LCO/Pt devices exhibits a high resistance ratio of $\sim 10^4$ between the high resistance state (HRS) and low resistance state (LRS) and exhibits excellent endurance/retention characteristics. The conduction mechanism of the HRS in the high voltage range is dominated by the Schottky emission, while the Ohmic conduction dictates the LRS and the low voltage range of HRS. The RS behavior in the Au/LCO/Pt devices can be understood by the formation and rupture of conducting filaments consisting of oxygen vacancies, which is validated by the temperature dependence of resistance and x-ray photoelectron spectroscopy results. Further analysis shows that the reset current I_R and reset power P_R in the reset processes exhibit a scaling law with the resistance in LRS (R_0), which indicates that the Joule heating effect plays an essential role in the RS behavior of the Au/LCO/Pt devices.

PACS: 73.40.Rw, 73.50.−h, 73.61.−r, 73.61.Ng DOI: 10.1088/0256-307X/35/4/047301

Resistive random access memory (RRAM) with a simple metal-insulator-metal (MIM) structure has been considered to be able to overcome the physical and technical limitations of conventional Si-based flash memory due to the outstanding features of high density, high switching speed, and low power consumption.[1−3] The resistive switching (RS) behavior is the underlying physical phenomenon behind the RRAM to store information. The resistance state of RRAM devices exhibits reversible transition between a high resistance state (HRS) and a low resistance state (LRS) under appropriate external electrical stimuli. The RS behavior can be classified into unipolar and bipolar types based on the polarity of the applied voltage for switching. In addition, the type of conducting path is also used to categorize the RS. One class shows a filamentary conducting path, in which the RS results from the formation and rupture of conducting filaments (CFs) in an insulating matrix. The other type of conducting path is an interface-type path, in which the RS takes place at the electrode/insulator interface.[4] The RS behavior has been observed in a wide range of materials such as oxides, chalcogenides, carbon-based materials, nitrides, and organic materials.[5−11] Especially, the oxygen vacancies in the oxide materials are the elemental point defects, which can disturb the ground state and can promote exotic functionalities at sufficiently high concentrations.[12] Therefore, the oxides are the front runner for developing next-generation energy and memory devices.[4,13]

Among the abundant oxides, the transition metal oxides with perovskite structure denoted as ABO_3 such as $SrTiO_3$,[6] Cr-doped $SrTiO_3$,[14] $BiFeO_3$,[15] $Pr_{1-x}Ca_xMnO_3$,[16] $La_{0.5}Sr_{0.5}CoO_{3-\delta}$,[17] $La_{1-x}Sr_xMnO_3$,[18] $BaTi_{0.95}Co_{0.05}O_3$,[19] $YCrO_3$,[20] and $SrFeO_x$[21] have attracted enormous attention for RRAM applications. The perovskite lattice can accommodate a large variety of cation ions with different ionic radii and valences as well as high concentrations of oxygen vacancies, which are propitious to optimize the performance of oxide-based RRAM devices.[22−24] Fu *et al.* have reported that the introduction of oxygen vacancies in the $La_{0.5}Sr_{0.5}CoO_{3-\delta}$ thin films can induce the bipolar RS behavior with excellent endurance and retention characteristics.[17] Yan *et al.* have demonstrated that $BaTi_{0.95}Co_{0.05}O_3$-based RRAM devices with high performance of RS characteristics can be obtained via engineering the concentration of oxygen vacancies.[19] Acharya *et al.* have found that $SrFeO_x$-based RRAM devices can exhibit excellent bipolar RS characteristics resulted from

*Supported by the Joint Funds of the National Natural Science Foundation of China and the Chinese Academy of Sciences' Large-Scale Scientific Facility under Grant No U1532149, and the National Basic Research Program of China under Grant No 2014CB931704.

**Corresponding author. Email: huling@issp.ac.cn; xbzhu@issp.ac.cn

© 2018 Chinese Physical Society and IOP Publishing Ltd

a local reversible phase transformation in $SrFeO_x$ thin films between brown millerite and perovskite structures due to the migration of oxygen vacancies.[21] $LaCrO_3$ (LCO)-based materials, belonging to the perovskite family, have gained interest for a variety of electrochemical applications such as the interconnector in a solid oxide fuel cell, catalytic, and oxygen separator membrane due to the possibility of tuning their electronic/ionic conductivity through doping La and Cr and subsequent formation of oxygen vacancies as well as the good stability over a wide range of oxygen atmospheres.[25–28] Theoretical studies point out that the formation energy of oxygen vacancies in the LCO is moderate among the $LaBO_3$ (B is $3d$ transition metal) series and the presence of oxygen vacancies in the LCO is energetically favorable under oxygen-poor conditions.[29,30] Furthermore, the LCO exhibits a small oxygen vacancy migration activation energy, which may facilitate the RS behavior.[31] These results indicate that the LCO thin films would be suitably used as the RS material to show good RS characteristics. In this study, the LCO thin films are deposited to construct RRAM devices and the corresponding RS behavior is investigated. It is found that the unipolar RS behavior in the Au/LCO/Pt devices exhibits the merits of a high resistance ratio between LRS and HRS, and exhibits excellent endurance/retention characteristics. The conduction mechanisms are the Ohmic conduction in LRS and the low voltage range of HRS, and the Schottky emission in the higher voltage range of HRS. The formation and rupture of CFs composed of oxygen vacancies are suggested to be responsible for the RS behavior in the Au/LCO/Pt devices. The existence of the scaling law between reset current (reset power) and the resistance in LRS (R_0) in the reset process indicates that the Joule heating effect plays an essential role in the RS behavior of the Au/LCO/Pt devices.

Polycrystalline LCO thin films were deposited on commercial Pt/Ti/SiO2/Si substrates by pulsed laser deposition. A polycrystalline LCO target was ablated by a KrF (248 nm) excimer laser (Coherent COMPexPro102) with an energy density of $2\,J/cm^2$ and a repetition of 5 Hz. The laser beam was focused onto the LCO target within a vacuum chamber. The base pressure of the vacuum chamber was about 1×10^{-3} Pa and high purity oxygen (99.999%) was injected into the chamber through a mass-flow controller (MFC, Seven star D07-7B). During the deposition, the substrate temperature was 600℃ and the oxygen pressure was 1 Pa. The distance between the LCO target and the substrate was kept at 5 cm. The Au top electrodes of 200 μm in diameter were deposited by dc-magnetron sputtering with a shadow mask. The current-voltage (I–V) measurements in top-bottom configuration by a Keithley 2400 source-meter unit were used to study the RS behavior of the Au/LCO/Pt devices. The structural properties of the LCO thin films were examined by means of x-ray diffraction (XRD, Philips X-Pert Pro MPD). The thickness of the LCO thin films was measured by a field emission scanning electron microscope (SEM, FEI Sirion 200). The surface morphological properties were checked by an atomic force microscope (AFM, Cypher ES). The chemical bonding states of the elements in the LCO thin films were obtained by x-ray photoelectron spectroscopy (XPS, Thermo ESCALAB 250) with monochromatic Al K ($hv = 1486.6$ eV).

The XRD pattern shown in Fig. 1(a) reveals that the LCO thin film has a polycrystalline structure. All the peaks can be assigned to the bulk LCO (JCPDS 24-1016). Figure 1(b) presents a cross-sectional SEM image of the LCO thin film deposited on the $Pt/Ti/SiO_2/Si$ substrate. The thickness of the LCO thin film is about 170 nm. The AFM topography image of the LCO thin film shown in Fig. 1(c) indicates that the surface of the LCO thin film is smooth and the root-mean-square roughness is about 2 nm.

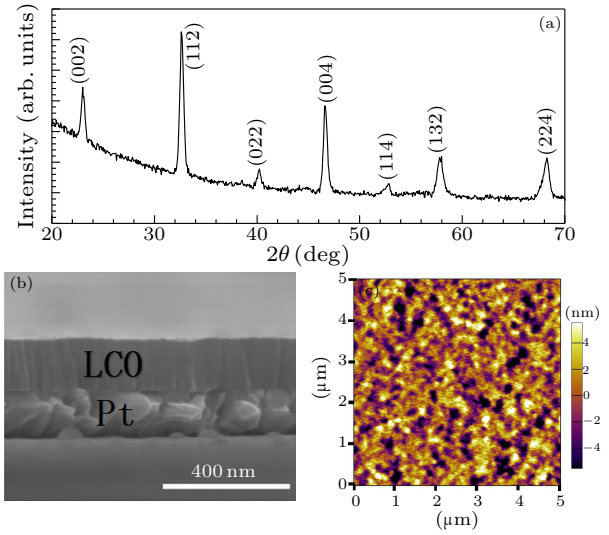

Fig. 1. (a) XRD pattern of the LCO thin film (grazing incidence) at room temperature. (b) The cross-sectional SEM image of the LCO/Pt/Ti/SiO_2/Si substrate without top electrode. (c) AFM topography image of the LCO thin film.

Figure 2(a) shows the typical I–V characteristics of the Au/LCO/Pt device obtained by the voltage sweeping mode. The positive voltage was applied on the Au top electrode and the Pt bottom electrode was grounded. Initially, the as-prepared Au/LCO/Pt devices were found to be insulating with the resistance value of ∼5 MΩ. A forming process was necessary to trigger the reproducible RS behavior. This process is

generally achieved by applying a soft breakdown electric field in the voltage sweeping mode with an appropriate compliance current (I_{CC}). During the voltage sweeping process, the current flowing through the device increased abruptly at ∼11.3 V, as shown in the inset of Fig. 2(a). The I_{CC} was 5 mA to prevent the device from permanent dielectric breakdown due to the high current flow in LRS. After the forming process, the Au/LCO/Pt device turned to LRS and exhibited reproducible RS behavior. Subsequently, as the voltage was swept from 0 to 1.3 V, an abrupt drop in the current was observed. This indicates the sudden increase of the device resistance and switching of the device from LRS to HRS, which is called the reset process. In HRS, as the voltage was swept again from 0 to 5 V, the abrupt increase of the current was observed and the device switched from HRS to LRS, which is called the set process. The set and reset operation can also be operated in the negative voltage direction. Therefore, the Au/LCO/Pt devices exhibit the unipolar RS behavior.

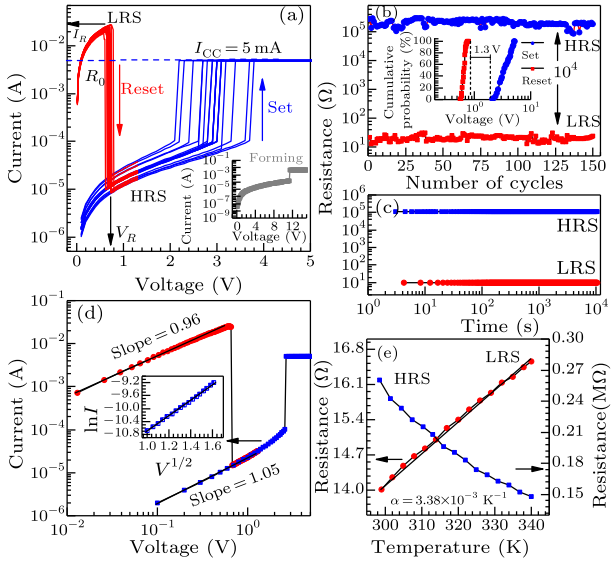

Fig. 2. (a) Reproducible I–V characteristic in a semilogarithmic scale of the Au/LCO/Pt device. Here R_0, I_R and V_R denote the resistance of the device in LRS, the reset current, and the reset voltage, respectively. The inset shows the I–V curve of the forming process. (b) The endurance performance of the Au/LCO/Pt devices. The resistance values are recorded under a small reading voltage of 0.1 V. The inset shows the statistical distributions of the set and reset voltages. (c) The retention characteristic of the devices at room temperature over a time period of 10^4 s. (d) The double logarithmic coordinates of LRS and HRS of the Au/LCO/Pt device. The inset shows the Schottky emission fitting of $\ln(I)$–$V^{1/2}$. (e) The temperature dependence of the resistance in LRS and HRS.

The reset and set processes have been repeated for 150 cycles to investigate the RS performance of the Au/LCO/Pt devices. The cycle-to-cycle resistance states and the switching voltages have been analyzed statistically. Figure 2(b) shows the endurance performance and the distribution of the resistance values of HRS and LRS under a small reading voltage of 0.1 V. The variation of HRS and LRS during a cycle is very small and the ratio of HRS and LRS is found to be ∼ 10^4 without degradation. The endurance measurement indicates that the RS behavior in the Au/LCO/Pt devices is highly reliable and reproducible. The distribution of the set and reset voltages is presented in the inset of Fig. 2(b). The set and reset voltages are found to vary in the ranges of 2.1–5.0 V and 0.58–0.80 V, respectively. These values of set and reset voltages exhibit a ∼1.3 V window of switching voltages between the HRS and LRS. Figure 2(c) displays the retention characteristic of HRS (after the reset process) and LRS (after the set process) under 0.1 V voltage for reading a current value at room temperature. Over a time period of 10^4 s, the resistance values of HRS and LRS are almost unchanged, which validates the nonvolatile RS behavior of the Au/LCO/Pt device.

The I–V curves are replotted in log-log scale in Fig. 2(d) to identify the conduction mechanism. The fitting is performed for both LRS and HRS in various voltage regimes and the straight lines are the fitting results. The I–V curve of LRS exhibits a linear relationship with a slope of ∼0.96, which indicates the Ohmic conduction behavior. This result can be ascribed to the formation of CFs during the set process. In contrast, the I–V curve of HRS can be divided into two ranges. In the low voltage range from 0 to 1 V, the current depends linearly on the voltage with a slope of ∼1.05, which shows the Ohmic conduction. However, at higher voltage the I–V curve shows nonlinear behavior. The nonlinear conduction mechanisms including the Schottky emission, the Poole–Frenkel emission, and space charge limited current were adopted to fit the nonlinearity of the I–V curve. It is found that the Schottky emission can fit best. The linear dependence of $\ln(I)$ versus $V^{1/2}$ is shown in the inset of Fig. 2(d). The Schottky emission originates from the thermal excitation by increasing the applied electric field.[32] The injected carriers can overcome the Schottky barrier at the interface and pass through the LCO at higher electric field in the HRS.[33] Figure 2(e) shows the temperature dependent resistances of HRS and LRS for the Au/LCO/Pt devices. The resistance of HRS decreases with increasing temperature, which could be ascribed to a typical semiconducting or insulating behavior. On the other hand, the resistance of LRS increases with increasing temperature, which is a typical metallic conducting behavior. The variation of the resistance in LRS with temperature can be

expressed by $R(T) = R_1(1 + \alpha(T - T_1))$, where R_1 is the resistance at T_1, and α is the resistance temperature coefficient. The value of α is determined to be $3.38 \times 10^{-3}\,\mathrm{K}^{-1}$ by a line fitting to the variation of the resistance in LRS with temperature. Similar values have been reported in $BaTi_{0.95}Co_{0.05}O_3$, $YCrO_3$, $Bi_{12}TiO_{20}$, $La_2Mo_2O_9$, and $SmGdO_3$-based RRAM devices, in which the CFs are composed of oxygen vacancies or metallic atoms.[19,20,34–36]

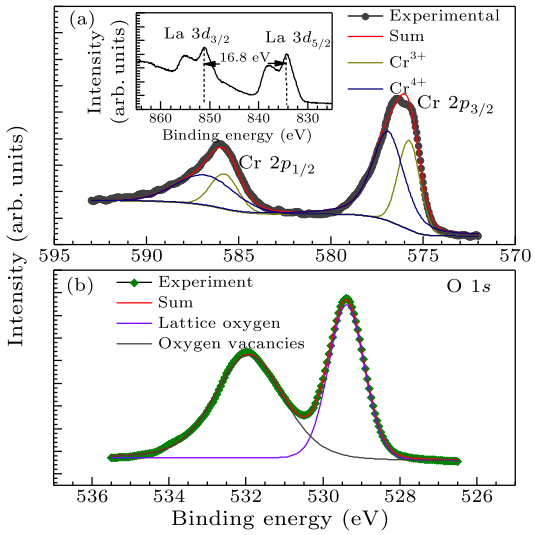

Fig. 3. XPS spectra of (a) Cr $2p$ and (b) O $1s$ of the LCO thin film (after several set/rest processes). The inset shows the XPS spectra of La $3d$ regions.

In light of the above experimental results, the RS behavior in the Au/LCO/Pt device can be explained by the CF (thermo-chemical) model. The CFs are firstly formed in the forming process. Subsequently, the formation and rupture of the CFs result in the reversible switching of the resistance states between HRS and LRS, which are corresponding to the set and reset processes, respectively. The formation of CFs is achieved through the alignment of high density of defects (mostly oxygen vacancies or metal interstitials) by high electric field during the forming and set processes.[37] In the reset process, the large current flowing through the CFs produces a significant Joule heating effect, which ruptures the CFs through the local Joule heating-induced redox in the LCO thin film. XPS analysis has been carried out to identify whether the oxygen vacancies or metallic atoms in the LCO thin film should be responsible for the RS behavior. The inset in Fig. 3 shows the XPS spectra of the La $3d$ region of LCO thin films and the valence of La can be determined to be +3 without reduced bonding signal. As shown in Fig. 3(a), the Cr exhibits multivalent states where Cr $2p_{3/2}$ and Cr $2p_{1/2}$ can be divided into two peaks corresponding to Cr^{3+} and Cr^{4+}, respectively.[20,38] Therefore, these results rule out the presence of any metallic component of either La or Cr, while Cr^{3+} should dominate in stoichiometric LCO, tetravalent Cr^{4+} may be formed by a charge compensation reaction due to the vaporization of Cr.[39] The element composition of the LCO thin film is determined as La:Cr:O≈1:0.94:2.96 by XPS. Figure 3(b) displays the O $1s$ XPS spectra of the LCO thin film, which consists of two peaks at binding energies of 529.4 and 531.8 eV. The former and the latter are assigned to lattice oxygen ions and non-lattice oxygen ions in the oxygen vacancies region, respectively.[40] The oxygen vacancies in the LCO thin film are expected to form at the oxygen-poor atmosphere during deposition.[30] Therefore, the oxygen vacancies would play an essential role in the RS behavior of the Au/LCO/Pt devices.

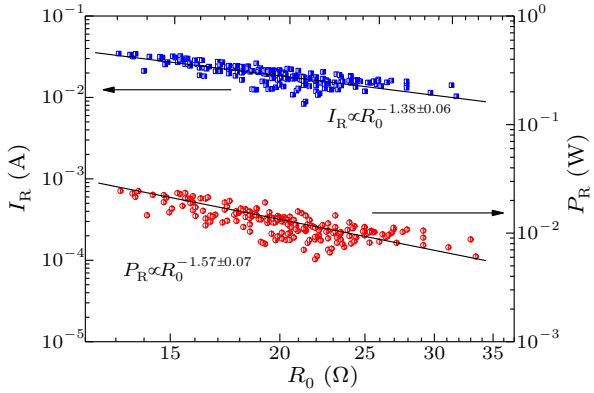

Fig. 4. The variation of reset current I_R and reset power P_R with R_0. The solid lines represent data fitting with a scaling law.

Figure 4 depicts both reset current (I_R) and power (P_R) as a function of R_0 in the reset processes. The value of P_R is defined as the product of I_R and reset voltage (V_R). It is clear that both I_R and P_R can be scaled by a power law of $I_R(P_R) \propto R_0^{-\beta(\gamma)}$ with exponents $\beta(\gamma)$ of 1.38 ± 0.06 (1.57 ± 0.07). These values are comparable with that of $La_2Mo_2O_9$, NiO, Nb_2O_5, and HfO_2-based RRAM devices.[36,41,42] The observed scaling law is consistent with the CFs (thermo-chemical) model. The large local current is constricted in the CFs of LRS and the consequent Joule heating increases with increasing the current during the voltage sweep process. The reset process will happen as the Joule heating can bring about the rupture of CFs through the thermo-induced redox reaction.[37] Since a larger R_0 value indicates weaker CFs, I_R and P_R needing to rupture the CFs are lower, as expected by the scaling law. Therefore, the scaling law indicates the importance of the Joule heating effect for the RS behavior of Au/LCO/Pt devices.

In summary, polycrystalline LCO thin films have been deposited on the Pt/Ti/SiO_2/Si substrates us-

ing pulsed laser deposition, and the RS characteristics of the Au/LCO/Pt device has been investigated. It is found that the Au/LCO/Pt device shows excellent unipolar RS characteristics with a high resistance ratio between HRS and LRS, good endurance and retention characteristics. The RS mechanism based on the filamentary (thermo-chemical) model can explain the RS behavior related to the migration of oxygen vacancies. The reset current ($I_{\rm R}$) and reset power ($P_{\rm R}$) in the reset process exhibit a scaling law with the resistance in LRS (R), which indicates the importance of the Joule heating effect for the RS behavior of Au/LCO/Pt devices.

References

[1] Waser R, Dittmann R, Staikov G and Szot K 2009 *Adv. Mater.* **21** 2632
[2] Shang D S, Sun J R, Shen B G and Matthias W 2013 *Chin. Phys.* B **22** 067202
[3] Pan F Gao S, Chen C, Song C and Zeng F 2014 *Mater. Sci. Eng.* R **83** 1
[4] Sawa A 2008 *Mater. Today* **11** 28
[5] Gao T T, Tan T T and Liu Z T 2015 *Chin. Phys. Lett.* **32** 016801
[6] Szot K, Speier W, Gihlmayer G and Waser R 2006 *Nat. Mater.* **5** 312
[7] Lai X B, Wang Y H, Shi X L, Li D Y, Liu B Y, Wang R M and Zhang L W 2016 *Chin. Phys. Lett.* **33** 067202
[8] Guo Z, Li M Q and Huang X J 2015 *Small* **11** 6285
[9] Zhou J W, Li T R, Zhang D, Ren B, Zhang S W, Huang J, Zhang J M, Wang L, Jiang Y C, Gao J and Wang L J 2017 *Vacuum* **135** 115
[10] Chen C, Yang Y C, Zeng F and Pan F 2010 *Appl. Phys. Lett.* **97** 083502
[11] Kim T W, Zeigler D F, Acton O, Yip H L, Ma H and Jen A K Y 2012 *Adv. Mater.* **24** 828
[12] Khare A, Shin D, Yoo T S, Kim M, Kang T D, Lee J, Roh S, Jung I, Hwang J, Kim S W, Noh T W, Ohta H and Choi W S 2017 *Adv. Mater.* **29** 1606566
[13] Kubicek M, Bork A H and Rupp J L M 2017 *J. Mater. Chem.* A **5** 11983
[14] Janousch M, Meijer G I, Staub U, Delley B, Karg S F and Andreasson B P 2007 *Adv. Mater.* **19** 2232
[15] Deng H L, Zhang M, Li T, Wei J Z, Chu S J, Du M Y and Yan H 2015 *J. Alloys Compd.* **639** 235
[16] Seong T, Choi K B, Seo I, Oh J, Moon J W, Hong K and Nahm S 2012 *Appl. Phys. Lett.* **100** 212111
[17] Fu Y J, Xia F J, Jia Y L, Jia C J, Li J Y, Dai X H, Fu G S, Zhu B Y and Liu B T 2014 *Appl. Phys. Lett.* **104** 223505
[18] Liu D Q, Wang N N, Wang G, Shao Z Z, Zhu X, Zhang C Y and Cheng H F 2013 *Appl. Phys. Lett.* **102** 134105
[19] Yan Z B, Guo Y Y, Zhang G Q and Liu M J 2011 *Adv. Mater.* **23** 1351
[20] Sharma Y, Misra P and Katiyar R S 2014 *J. Appl. Phys.* **116** 084505
[21] Acharya S K, Nallagatla R V, Togibasa O, Lee B W, Liu C, Jung C U, Park B H, Park J, Cho Y, Kim D, Jo J, Kwon D, Kim M, Hwang C S and Chae S C 2016 *ACS Appl. Mater. Interfaces* **8** 7902
[22] Pena M A and Fierro J L G 2001 *Chem. Rev.* **101** 1981
[23] Waser R and Aono M 2007 *Nat. Mater.* **6** 833
[24] Shi T, Chen Y P and Guo X 2016 *Prog. Mater. Sci.* **80** 77
[25] Fergus J W 2004 *Solid State Ionics* **171** 1
[26] Kaddouri A, Ifrah S and Bergeret G 2009 *Catal. Lett.* **129** 336
[27] Larring Y, Vigen C, Ahouanto F, Fontaine M, Peters T, Smith J B, Norby T and Bredesen R 2012 *Biochim. Biophys. - Acta Biomembr.* **2** 665
[28] Zenou V Y, Fowler D E, Gautier R, Barnett S A, Poeppelmeier K R and Marks L D 2016 *Solid State Ionics* **296** 90
[29] Su H Y and Sun K J 2015 *J. Mater. Sci.* **50** 1701
[30] Dabaghmanesh S, Sarmadian N, Neyts E C and Partoensa B 2017 *Phys. Chem. Chem. Phys.* **19** 22870
[31] Cherry M, Islam M S and Catlw C R A 1995 *J. Solid State Chem.* **118** 125
[32] Hu W, Zou L L, Chen R Q, Xie W, Chen X M, Qin N, Li S W, Yang G W and Bao D H 2014 *Appl. Phys. Lett.* **104** 143502
[33] Chiu F 2014 *Adv. Mater. Sci. Eng.* **2014** 578168
[34] Chen R Q, Hu W, Zou L L, Xie W, Li B J and Bao D H 2014 *Appl. Phys. Lett.* **104** 242111
[35] Hu L, Lin G T, Luo X, Wei R H, Zhu X B, Song W H, Dai J M and Sun Y P 2016 *J. Appl. Phys.* **120** 215303
[36] Sharma Y, Misra P, Pavunny S P and Katiyar R S 2014 *Appl. Phys. Lett.* **104** 073501
[37] Kim K M, Jeong D S and Hwang C S 2011 *Nanotechnology* **22** 254002
[38] Zhang K H L, Du Y, Sushko P V, Bowden M E, Shutthanandan V, Sallis S, Piper L F J and Chambers S A 2015 *Phys. Rev.* B **91** 155129
[39] Bonet A, Baben M, Travitzky N and Greil P 2016 *J. Am. Ceram. Soc.* **99** 917
[40] Guo D Y, Wu Z P, An Y H, Li P G, Wang P C, Chu X L, Guo X C, Zhi Y S, Lei M, Li L H and Tang W H 2015 *Appl. Phys. Lett.* **106** 042105
[41] Kim S I, Sa Y H, Kim J, Chang Y W, Kim N, Kim H and Yoo K 2014 *Appl. Phys. Lett.* **104** 023513
[42] Kim J, Jung K, Kim Y, Jo Y, Cho S, Woo H, Lee S, Inamdar A I, Hong J, Lee J, Kim H and Im H 2016 *Sci. Rep.* **6** 23930